JOURNAL OF AIRCRAFT
Vol. 44, No. 6, November–December 2007

Aerodynamic and Mission Performance of a Winged Balloon Guidance System

Kerry T. Nock,* Kim M. Aaron,† Matthew K. Heun,‡ and Alexey A. Pankine§
Global Aerospace Corporation, Altadena, California 91001-5327

DOI: 10.2514/1.31922

A winged balloon guidance system exploits the natural wind-field variation with the altitude available in planetary atmospheres to generate passive lateral control forces on a balloon using a tether-deployed aerodynamic surface below the balloon. Several balloon guidance system topics are discussed, including development status, physics and aerodynamics, systems performance, concept of operations, and the near-space applications of this technology for scientific, communications, and defense applications.

I. Introduction

BALLOON guidance systems (BGS) have been under development by Global Aerospace Corporation (GAC) for use by NASA's scientific balloon program. Several NASA-funded studies have also explored the BGS use for guiding scientific balloons on Mars, Venus, Titan, and the outer planets. In 2001, GAC carried out a scale-model flight test that validated the aerodynamics, stability, control, and operation of the BGS in a relevant environment, giving high confidence that a full-scale system will perform as expected on stratospheric Earth balloons. In addition, a full-scale mechanical prototype has been constructed that could be made ready for a flight demonstration.

A winged BGS exploits the natural wind-field variation with the altitude available in planetary atmospheres to generate passive lateral control forces on a balloon using a tether-deployed aerodynamic surface below the balloon. One embodiment of a BGS uses a wing suspended several kilometers below the balloon on a very long tether. In planetary atmospheres, there is generally a vector wind difference between two altitudes, separated by a few kilometers, which results in a relative wind at the wing, allowing it to generate a lift force. This lift force can be directed horizontally across the natural flight path of the balloon. This force is transmitted along the tether to the balloon, causing the balloon to drift across the winds at its altitude. Acting over long durations, this force can move the balloon hundreds to thousands of kilometers away from where it would have gone by simply drifting with the prevailing winds. A BGS enables a stratospheric balloon to control its latitude of operation, avoid high-population zones, and to target termination and landing to safe areas. As will be discussed, a winged BGS provides the best and most efficient technology available for guiding high-altitude balloons, based on data from prototype test flights and experimental data.

II. System Development Status

GAC has been developing a latitude trajectory control device, called a balloon guidance system (BGS), initially for the NASA Balloon Program Office (BPO) Ultra-Long-Duration Balloon (ULDB) project and later for potential commercial and defense customers. Design goals of the ULDB project are to carry a suspended mass of up to 2750 kg for 100 days at constant density altitude over 33.5 km. The specific innovation of this BGS concept is the exploitation of natural wind-field variation with altitude to generate passive lateral control forces on a balloon using a tether-deployed aerodynamic surface beneath the balloon. Under NASA's Small Business Innovation Research (SBIR) program Phase II funding, GAC built the full-scale mechanical prototype of the system shown in Fig. 1.

The SBIR work has prompted several scientist-driven, NASA-funded studies and numerous reports on the feasibility and performance of the concept for guiding Earth and planetary balloon systems. NASA resources outside the BPO and the SBIR program have been spent in assessing its performance, studying advanced designs, evaluating its use for guiding constellations of balloons, and for examining its capability for navigating balloons on other planets. The next step in development is the flight test demonstration of a prototype BGS in a relevant environment. This will require adding electronics, radios, mechanisms, and controls to the mechanical BGS wing assembly already built and developing a flight demonstration the BGS gondola interface package, including a winch system, controls, and radios.

This paper documents recent technical research into the mission performance of the BGS. This research, based on data from prototype test flights and experimental data, confirms that a winged BGS provides the best and most efficient technology known to be available for guiding high-altitude balloons.

In the following sections, we will explore the physics of operation, aerodynamic and systems performance, concept of operations, and many near-space applications of BGS technology.

III. Physics of Operation

We first begin with a simplified description of the operation of the BGS followed by a more complete description that includes most of the important physics. A winged BGS exploits the natural wind-field variation with altitude to generate passive lateral control forces on a balloon using a tether-deployed aerodynamic surface below the balloon. A lifting device, such as a wing on end, is suspended on a tether well beneath the balloon to take advantage of this variation in wind velocity with altitude. The wing generates a horizontal lift force that can be directed over a wide range of angles. A BGS consists of an aerodynamic system or "BGS wing" (e.g., near-vertical wing, support boom, and rudder) below the balloon, a 1-km-long tether and a winch system for lowering, and sometimes raising, the BGS wing. A variety of concepts for the aerodynamic system have been studied, including kites, dual-wing airfoils, and whirligigs [1]. Figure 2 illustrates the principle of operation of a single-wing BGS.

For the Earth applications, the balloon would typically be at 35-km altitude and the BGS main wing would be at 20-km altitude. Generally, there is a wind difference between altitudes that translates

Presented as Paper 2603 at the AIAA Balloon Systems Conference, Williamsburg, VA, 21–24 May 2007; received 2 May 2007; revision received 27 June 2007; accepted for publication 3 July 2007.

*President. Senior Member AIAA.
†Senior Engineer.
‡Senior Engineer. Member AIAA.
§Project Scientist.

Fig. 1 Full-scale mechanical prototype winged balloon guidance system.

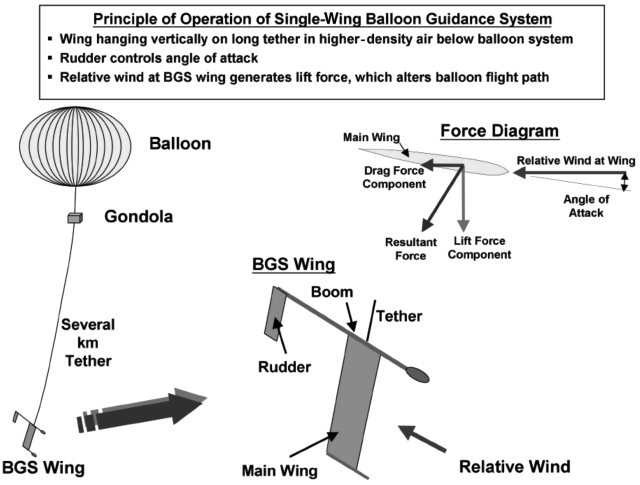

Fig. 2 Principle of operation of single-wing balloon guidance system.

to a relative wind on the BGS wing as it is dragged along by the balloon. This relative wind generates a lift and drag force at the wing, resulting in a horizontal force. Changing the angle of attack (AOA) of the wing by use of the rudder can modify the direction and magnitude of this force. This force, transmitted to the balloon by a tether, alters the balloon's path, providing a bias velocity of a few meters per second to the balloon drift rate. Features of a winged BGS include the ability to 1) passively exploit natural wind conditions, 2) operate day and night without energy storage, 3) control the direction of the balloon flight path in various wind conditions, 4) be made of lightweight materials and inflatable structures, and 5) operate with very little power and without consumables.

In usual wind circumstances with conventional designs, a balloon with a BGS cannot keep station over a given location. However, advanced BGS design concepts currently under study by Global Aerospace Corporation may be able to station-keep stratospheric airships.

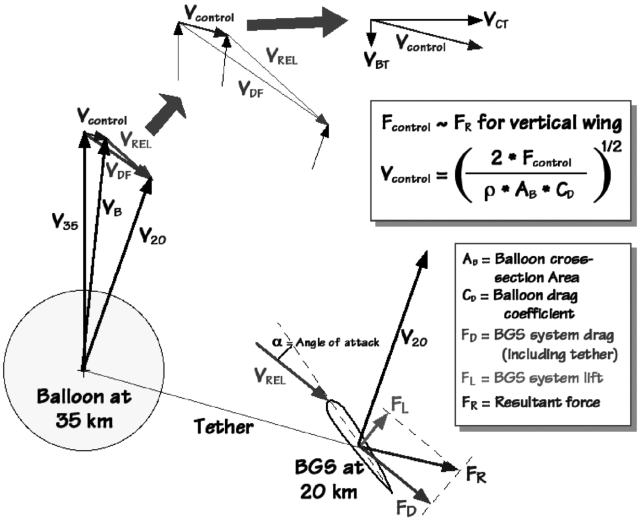

Fig. 3 BGS vector diagram illustrating its operation.

In reality, the BGS wing, tether, and balloon are affected by drag and inertial forces that need to be overcome. In addition, the system eventually comes to an equilibrium state in which all the forces are in balance. Next, we will describe this more complete, and complex, operation of the system. Later, we will apply specific example environmental and system parameters and calculate the example performance and characterize the overall system (balloon and BGS) state.

Figure 3 shows a vector diagram illustrating the wind vectors and dominant forces during operation of a winged BGS. The definitions of the various vectors are described in Table 1. The view is looking down from above the balloon and the BGS and is not to scale. The BGS (represented as an airfoil section) is at a much lower altitude than the balloon (represented by the circle). For illustration purposes, the BGS wing is shown much larger than it would be in proportion to the balloon. The upper portion of the figure shows expanded views of some small vector details.

Many simplifying assumptions are present in the vector diagram; however, the complex models that have been developed to characterize and simulate winged BGS behavior do not share these limitations. For example, the tether is shown here as a straight line. In reality, due to the variation in relative wind and atmospheric density along its length, the drag forces on the tether will cause it to have a gentle curvature. The detailed models include this effect by breaking the tether down into shorter segments over which conditions are treated as being constant. In Fig. 3, the tether drag force is shown to act at the BGS. This is not a bad assumption because the drag on the lower 10% or so of the tether dominates the rest of the tether, because the atmospheric density is greatest and the relative wind is also greatest here. The wing is assumed to be exactly vertical so that the lift and drag forces act in a horizontal plane. In actual operation, the wing will hang with some tilt to the side and backward. Our detailed models resolve the forces in three dimensions and include this effect. As the wing swings away from vertical, it also swings upward, following the end of the fixed-length tether. This causes three small reductions in the effective force applied. First, the wing is in slightly lower density air. Second, if the wind speed varies monotonically from the wing altitude to the balloon, there will be slightly less wind difference available. Third, the wing will be tilted a little from vertical, and so the horizontal component of force will be reduced (cosine effect). All of these effects are included in the more complex models and fractionally reduce the predicted performance. However, global and seasonal variations in the winds cause much larger effects on performance.

The system is assumed to be in equilibrium, so that the vector sum of the forces must equal zero. In the vertical direction, the buoyancy

Table 1 Notation shown in the vector diagram

V_{35}	Wind velocity (relative to the ground) at balloon altitude (35 km)	V_{CT}	Cross-track velocity component of $V_{control}$ (perpendicular to V_{35})
V_{20}	Wind velocity at the BGS wing altitude (20 km)	V_{BT}	Back-track velocity component of $V_{control}$ (parallel to V_{35})
V_B	Velocity of the balloon relative to the ground equals the velocity of all parts of the system	F_L	Lift force on the BGS wing (acts horizontally and is perpendicular to V_{REL})
$V_{control}$	Control velocity of the balloon due to action of the BGS ($V_B - V_{35}$)	F_D	Drag force on the BGS wing (acts horizontally and is parallel to V_{REL})
V_{REL}	Relative wind velocity at the BGS ($V_B - V_{20}$)	F_R	Resultant force on BGS = $F_L + F_D \sim$ drag force on the balloon
V_{DF}		$F_{control}$	Drag force on the balloon due to $V_{control} \sim F_R$

force provided by the balloon exactly equals the weight of the system. These vertical forces are not shown in the diagram. When the wing swings up to one side, the lift force has a small upward component (sine of the hang-off angle), which would result in a small increase in the equilibrium altitude of the balloon, but this is a very small effect. The aerodynamic drag force on the balloon is equal to and opposite to the resultant aerodynamic force on the BGS (including the tether drag force). With this simplification, one can calculate the control velocity $V_{control}$ of the balloon (inset box in Fig. 3), in which A_B is the projected area of the balloon (as viewed from the side), C_D is the drag coefficient of the balloon (for flow from the side), and ρ is the atmospheric density at the altitude of the balloon. The angle of attack α of the BGS wing is controlled by adjusting the incidence angle of the rudder (not shown) and is usually arranged to produce close to the maximum lift coefficient for the wing, because this typically produces maximum useful control effect for the system. A small amount of iteration is required to determine the drift velocity vector that balances the forces, thereby making the system self-consistent or in equilibrium. The diagram in the figure is drawn to illustrate an equilibrium solution.

If we take a particular set of example environmental and BGS design parameters, we can calculate its example performance. We should first emphasize that these performance values assume a fully balanced equilibrium solution that requires iteration until forces are balanced. There is no single calculation of control velocity, given winds at the balloon and the BGS wing; however, we can show that the solution is self-consistent. We first assume that the balloon is flying at 35-km altitude in January at the latitude of Alice Springs, Australia, a typical scientific balloon launch site. Given this latitude and season, the mean winds [2] V_{35} and V_{20} are 29.5 and 5.5 m/s, respectively, which we take to be parallel in this calculation, for simplicity. At 35-km altitude, the air density ρ_{35} is 0.00846 kg/m^3. Also, the drag coefficient of the balloon, C_D, is assumed to be equal to 0.2, an expected value after the equilibrium speed is reached. We also assume that the balloon radius R_B is 50 m and that the BGS has a lift coefficient C_L of 1.0 at an AOA of 12.7 deg; a drag coefficient at zero AOA, C_{D_0}, of 0.08; Oswald's efficiency factor e of 0.6; a wingspan b of 5.5 m; a chord c of 1.1 m; a wing aspect ratio AR of 5; and that the tether is 15 km long.

For these conditions, we calculate the velocities for which the forces are balanced. For this self-consistent solution (force-balanced), the relative wind on the BGS wing, V_{REL}, is 21.12 m/s, the cross-track system velocity V_{CT} is 3.36 m/s, a back-track velocity V_{BT} is 3.15 m/s, and the resultant control velocity $V_{control}$ is 4.61 m/s. If the balloon were free-floating at 35-km altitude, it would simply drift at the wind speed of 29.5 m/s in whatever direction the wind was blowing. With the forces from the BGS (transmitted via the tether) acting on the balloon, it is slowed down by 3.15 m/s and moves across the prevailing winds with a speed of 3.36 m/s. Now we shall illustrate the self-consistent solution for $V_{control}$, which we know to be 4.61 m/s from our model. At the BGS wing, the air density ρ_{20} is 0.0889 kg/m^3, about a factor of 10 higher than at 35-km altitude. This higher density is a decided advantage for the tiny wing compared with the balloon. First we calculate the lift L and drag D of the BGS wing and tether that are a function of the relative velocity at the wing, the aerodynamic characteristics of the BGS wing, and the air density at 20-km altitude. Lift is given by

$$L = 0.5\rho_{20}V_{REL}^2 C_L bc$$

which, for the preceding values, is 120 N.

The drag of the BGS system is composed of the drag of the wing and the drag of the tether. For this simplified model calculation, the drag of the tether is distributed all along the length of the tether in 500-m-long segments. Because the air density is a factor of 10 higher at the bottom, the lower part of the tether dominates the tether drag component of the system drag. We can approximate the system drag from $D_{system} = D_{wing} + D_{tether}$, where wing drag is given by $D_{wing} = 0.5\rho_{20}V_{REL}^2 C_{Dwing} bc$, where $C_{Dwing} = C_{D_0} + (C_L^2/\pi eAR)$.

In this approximation, the tether drag is $D_{tether} = 0.5 \cdot C_{Dtether} \cdot \ell d \sum \rho_i V_{REL_i}^2$, where the tether segment length ℓ is 500 m, the tether diameter d is 1 mm, and the assumed tether drag coefficient $C_{Dtether}$ is 1.0. For the conditions and parameters described previously, the tether drag contribution is roughly 57 N, the BGS wing drag is 22.3 N for a total BGS system drag of 79 N, and the wing lift is 120 N. If we calculate the approximate resultant force, $(120^2 + 79^2)^{0.5}$, it comes to 143 N. The exact value of the drag on the balloon is $D_B = 0.5\rho_{35}V_{REL}^2 C_{D_B} A_B$, or only 141 N, which is exactly equal to our computer calculation of resultant BGS forces and very close to the approximate value of the resultant force in the preceding simplified calculation. The reason these numbers do not match exactly is that the drag on the tether is really acting in different directions along the length of the tether and the simple hand calculation does not add these forces vectorially as does the computer model.

Despite the very large size of the balloon, it takes a surprisingly small amount of force to produce these drift speeds, due to the very low density of the atmosphere. In contrast, the buoyancy force $F_{buoyancy}$ is given by the weight of air displaced. This can be calculated by multiplying the volume of the balloon by the air density at its altitude and by the acceleration due to gravity:

$$F_{buoyancy} = \rho \cdot g_0 \tfrac{4}{3}\pi R_{balloon}^3$$

where $g_0 = 9.80665$ m/s^2.

At 35-km altitude, the air density is 0.00846 kg/m^3, and so the mass of air displaced is 4430 kg, hence the buoyancy force is 43,440 N. The very small horizontal drag force of 141 N on the balloon applied at the bottom of the flight train will cause an insignificant tilt of the balloon of $\sim$0.2 deg.

It is only slightly more complicated to check the vector geometry to be certain that the magnitude of the relative velocity at the wing is 21.12 m/s, as calculated in the computer model. One would expect it to be close to the wind-speed difference between the two altitudes minus the back-track (slowing down) velocity of the system. Hence, the relative wind at the wing should be about 29.5 m/s $-$ 5.5 m/s $-$ 3.15 m/s $=$ 20.85 m/s. The little extra in the actual relative velocity is due to the cross-track velocity of 3.36 m/s adding in the perpendicular direction. So the relative wind would be adjusted to $(20.85^2 + 3.36^2)^{0.5} = 21.12$ m/s, which agrees exactly with the model.

Given a wing mass of 90 kg (weight of 883 N), the wing will pull the tether to one side to an angle of about $\tan^{-1}(120 \text{ N} \div 883 \text{ N}) =$ 7.74 deg. The drag on the wing and tether will pull it back a somewhat smaller amount. This angle is so small that the altitude of the wing will not change appreciably, nor will the horizontal

component of the lift vector be reduced significantly. The wing will swing to one side a distance of $15,000\ \text{m} \times \sin(7.74\ \text{deg}) = 2020\ \text{m} = 2\ \text{km}$, but it will climb only $15,000\ \text{m} \times [1 - \cos(7.74\ \text{deg})] \sim 136\ \text{m}$, not far enough to be worth correcting the air density. The vertical component of the slightly tilted wing will be $120\ \text{N} \times \sin(7.74\ \text{deg}) = 16\ \text{N}$. Contrast this with the buoyancy force of 43,440 N and it will be clear why we usually do not bother to estimate the slight increase in equilibrium altitude of the system.

So far, everything discussed assumes the system is in equilibrium. Let us use some simple hand calculations to get an idea of the time scales involved with getting the system from a starting point to this equilibrium state. For this example, the horizontal component of the combined lift and drag forces (added vectorially) is about 141 N. For a buoyant system in equilibrium, the system mass is equal to the mass of air displaced, which was calculated earlier to be 4430 kg. This includes all mass of the system, including the helium lifting gas, the balloon envelope, the payload, the tether, and the BGS wing. When a sphere is accelerated through a fluid, additional force is required to accelerate the displaced flowfield around the sphere. For a sphere, one typically accounts for this by adding a virtual mass, or added mass, equal to half the mass of the fluid displaced. This result comes from integrating momentum in the flowfield using potential flow past a sphere. Therefore, the total effective mass to be accelerated in our case is 6645 kg. A force of 141 N accelerating a mass of 6645 kg produces an acceleration of $0.021\ \text{m/s}^2$. The total change of velocity is 4.61 m/s. If the force acted constantly, the time it would take to bring about this change of velocity would be $4.61\ \text{m/s} \div 0.021\ \text{m/s}^2$ or 220 s or about 3.6 min. Of course, the balance of forces changes as the drag on the balloon builds up as the system accelerates, and so it will actually take longer than this to reach equilibrium. If we assumed it to be an exponential approach (which it is not, due to the nonlinearities involved), then this 220-s time period would actually be one time constant[¶]. So it would really take closer to 10 min for the system to be effectively in equilibrium. Given that we are envisioning flights of many days or months, this short time period is not important to the BGS operation. In our simulations, we typically use time steps of 1–6 h. But conditions in the atmosphere vary so slowly that the commanded operation may persist for days. In the rare circumstance that the wing is commanded to change the direction of pull to the opposite side, there is also a finite time for the wing to fly the couple of kilometers from one side to the other at the end of its 15-km pendulum. If we allowed it to, it could easily travel across this distance at speeds of 50–100 m/s, taking perhaps 30 s total. It is our preference to adjust the angle of attack slowly, keeping the system in quasi equilibrium the whole time. We can select a time for this to happen, but it would have to be on the order of a few time constants, and so again, it is a relatively short time compared with times of interest.

IV. Aerodynamic Performance

In this section, we will discuss the selected BGS airfoil lift performance as a function of Reynolds number, our scale-model test results, and possible lift-enhancement options.

A. Airfoil Performance

A BGS wing operates at low speeds and at very high, low-air-density, altitudes. The characteristics of its environment, combined with its physical size, result in a relatively low Reynolds number for operation (40,000 to 200,000) compared with typical aircraft operation (greater than 10^6). Because most airfoil research deals with high Reynolds numbers, most of the information on lift and drag performance of airfoils is for high-Reynolds-number operation. There is, however, a surprising amount of data, both experimental and model predictions, dealing with low-Reynolds-number operation of the wing selected for the BGS: namely, NACA[**] 0015. The 0015 designation refers to a symmetric wing having a thickness of 15% of its chord length.

1. Airfoil Selection

In 1999, at the time of our SBIR Phase I effort, we had very crude estimates of airfoil performance, because we had not selected an airfoil for the full-scale system. The airfoil for our scale model was an NACA 0015, because it had been available in an almost-ready-to-fly (ARF) model kit at the time we built the system and was a reasonable and representative selection at the time.

In 2000, after considerable research and calculation, we selected a NACA 0015 airfoil section for our full-scale test wing and rudder. Coincidentally, it was the same airfoil section as our scale model that was originally built in 1999. At the time of its selection, we found some decent data for several airfoils (but not NACA 0015) for the Reynolds number close to our nominal operating point (around 70,000). After examining some of the data, we concluded that most of the low-Reynolds-number airfoils are really designed to minimize drag near a fairly low design lift coefficient. This would correspond to a typical cruising condition, and low drag means low fuel consumption. We were only somewhat concerned about drag, but we did care about getting a large lift force.

When airfoil designers want to achieve a high lift coefficient, they use highly cambered (asymmetric) airfoils, and so we selected a symmetric section that could be used to generate a lift force to the right or the left from a vertical position. Historically, airfoil designers seem not to have paid much attention to achieving maximum lift coefficient for symmetric sections at low Reynolds numbers.

Available data show that relatively thin airfoils stall at lower lift coefficients than thicker airfoils, and so we selected a relatively thick airfoil (15% of the chord). Other than this general trend with thickness, based on the experimental data we saw, the maximum lift coefficient for symmetric airfoils does not seem to depend tremendously on the particular airfoil shape. As the airfoil gets thicker, the drag starts to increase, and so designers lose interest and tend not to test thick sections experimentally very often.

2. Early Lift-Performance Estimates

Early in the development of the winged BGS concept, rough estimates of the maximum lift coefficient of the BGS airfoil, before its actual selection, were between 1.2 and 1.4. At various points in the BGS development, we generated simulations of BGS performance using maximum lift coefficients between 1.0–1.4. After we selected our airfoil for the full-scale system, we estimated that we might achieve a lift coefficient near 1.0, but more likely at 0.8 or so. But this is for operation at low Reynolds numbers, which corresponds to $\sim 10\ \text{m/s}$ relative airspeed at float altitude on Earth. If the wind speed goes up to 20 m/s, then we estimated that we would easily be able to get section lift coefficients of 1.0. In relatively light surface winds, our scale model was estimated be at the same Reynolds number as our full-scale model, and so we thought we would be able to confirm this behavior with our scale model, although it was not the primary objective of the scale-model testing. In our second scale-model flight test in April 2001, which met its primary objective to confirm that there was no undesirable dynamic behavior, we did measure the lift coefficient to be 1.2 of the combined system (wing, rudder, boom, and associated hardware). We were a little surprised that this number was higher than early lift coefficient estimates of just the wing (0.8–1.0), but felt it was well within the level of uncertainty of both the experimental measurement and the early estimates, and because this was a combined system, lift coefficient could easily be higher.

3. Lift Performance of the NACA 0015 Airfoil

One can examine model predictions and experimental data to assess the lift performance of the subject airfoil. However, how good

[¶]This is a very interesting general result, left to the reader to confirm, that for any exponential approach to a constant, the initial slope projected to the final value works out to exactly one time constant.

[**]NACA was the predecessor to NASA. NASA, among other things, conducted researched on the performance of a variety of wing designs.

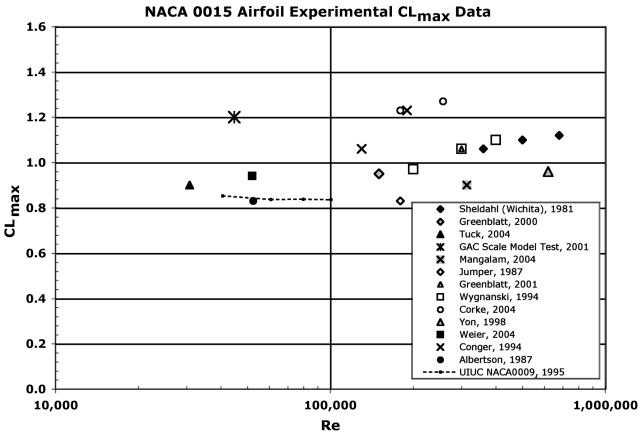

Fig. 4 Experimental measurements of NACA 0015 lift performance.

are model predictions for the Reynolds number range of interest? According to Wygnanski,[††] even modern model lift-performance computations are not reliable for low Reynolds numbers (in particular, for $Re < 50,000$), because airfoil characteristics are very sensitive to the location of the laminar-to-turbulent transition point, which depends greatly on surface quality and freestream turbulence in this Reynolds number range. Because the Reynolds number of interest is on the order of 40,000 to 200,000, we focus on the available experimental data.

Figure 4 summarizes historical experimental lift-performance measurements [3–14] of the NACA 0015 airfoil over the past 25 years. Some of the data are the result of experiments of lift-enhancement devices and techniques (electrostatic, oscillations, and pressure forcing). The measurements of interest to us are those baseline measurements when there are no lift enhancements in operation. About half the measurements occur in water tunnels. This figure contains only experimental results, no computer simulations or extrapolations. This figure illustrates two points:

1) There is considerable scatter in the experimental lift data (± 0.2), which has been recognized by a number of researchers.

2) There is no dramatic fall off in performance for $Re < 100,000$. The University of Illinois at Urbana–Champaign (UIUC) NACA 0009 data,[‡‡] which were very carefully collected, are included because they represent a floor of lift performance below which the NACA 0015 should never descend, assuming an identical experimental setup. A floor of performance is established, because at lower Reynolds number, thinner airfoils (e.g., NACA 0009) stall at lower angles of attack than thicker airfoils.

The scatter in the data is not surprising to experts in the field, because airfoil stall characteristics are very sensitive to the transition from laminar to turbulent flow in the boundary layer, which depends on airfoil surface quality and the quality of the flow tunnel in which the airfoil is tested. In fact, several of these experiments included surface features that were intentionally included to encourage this transition from laminar to turbulent flow in the boundary layer, which would delay flow separation and allow a greater maximum (stall) lift coefficient to be achieved. Although all the results presented here are baseline measurements with these lift-enhancement features turned off, in some cases, the residual surface imperfections unavoidably present due to the mounting of these features very likely improved the maximum lift coefficient a little over an ideal bare, very smooth, and symmetric airfoil. These features can and do "trip" the boundary layer, inducing turbulence that allows the boundary layer to remain attached at a higher AOA that results in improved lift performance. As we will discuss later, if improvement is desired, such boundary-layer-tripping features can be very easily added to the BGS airfoil.

The experimentally determined stall lift coefficient for the scale-model BGS is higher than the experimental data from the literature. This number could be somewhat higher than expected because of the high-turbulence environment of the outdoor test combined with the fact that the test actually measured the total lift coefficient of the entire BGS, not just the main wing airfoil. This will be discussed in more detail later.

B. Scale-Model Testing

In 1999 and 2001, GAC conducted experiments in which we operated, in windy conditions, a scale-model BGS suspended below a blimp tethered to the ground. The winds simulated the relative wind that the full-scale wing would experience, caused by the wind difference between a balloon at 35 km and the wing at 20-km altitude. The primary purpose of the first test, using an uninstrumented scale model, was to investigate the dynamic behavior of the BGS wing assembly with different overall configurations (e.g., canard versus conventional) and c.g. locations. In April 2001, GAC performed additional testing with several instruments mounted on the model to allow qualitative measurements to be made.

The objectives for this second scale-model test (SMT) were as follows:

1) Determine the most desirable location for the BGS wing-assembly center of mass.

2) Confirm the correct operation of all sensors.

3) Confirm transmission of data from the wing assembly to the ground.

4) Collect a sufficient quantity of data to analyze wing-assembly response to changes in rudder angle.

5) Demonstrate stability of the wing assembly.

6) Demonstrate the ability to vary the angle of attack of the wing assembly by remote control.

7) Demonstrate survival of all flight elements for a duration of 10 h of flight.

The primary objective of the test was to discover any aerodynamic instability problems, if they existed, which we did not find. Though the primary intent of the SMT was to investigate dynamic motions of the test article, and not particularly to measure the lift coefficient, we were able to infer some values of lift coefficient.

Figure 5 illustrates the design of the scale model that was tested. For reference, the main wing chord is 0.308 m.

Table 2 lists the dimensional analysis scaling relationships for the SMT compared with the full-scale system. Note that the average Reynolds number of the model actually flown was very close to that expected during flight of the full-scale system that was built. Because winds did vary during the scale-model test, the Reynolds numbers actually ranged between about 40,000 and 120,000, which roughly corresponds to the lower range of Reynolds number one would see for the operational full-scale system. Figure 6 displays the lift coefficient as a function of angle of attack during the testing. Reviewing the detailed data gathered during this test, the average Reynolds number during this lift versus AOA measurement was about 72,000. However, because the winds did vary during this measurement, the average Reynolds number during the measurement of the maximum lift coefficient point (1.2 at an AOA of about 12 deg) was actually about 45,000.

What we tested in April of 2001 was a complete system comprising a main wing, a rudder, a support boom, and various other appendages. It would not be surprising that this combined system has a higher combined coefficient of lift than a bare airfoil in a wind tunnel, because the rudder and the boom all contribute to the lift of the system, as would be true in a full-scale system. It really is not appropriate to directly compare the overall system lift coefficient with lift coefficients for isolated airfoil sections. To avoid potential confusion, we will state explicitly that the lift on the rudder is positive, not negative. The rudder here is analogous to the horizontal stabilizer for an aircraft. For most airplanes, the wing is cambered and the lift on the horizontal stabilizer is negative, countering the nose-down moment, at least at small angles of attack. With the symmetric airfoil used on the winged BGS, the moment about the quarter-chord point is zero. The system center of mass is behind the wing quarter-chord, and so the lift on the rudder has the same sign as the lift on the wing to balance moments about the center of mass. Hence, the rudder

[††]Personal communications with I. Wygnanski, 11 October 2006.

[‡‡]Data available online at http://www.ae.uiuc.edu/m-selig/pub/LSATs/vol1/N0009.LFT, [retrieved 2 May 2007].

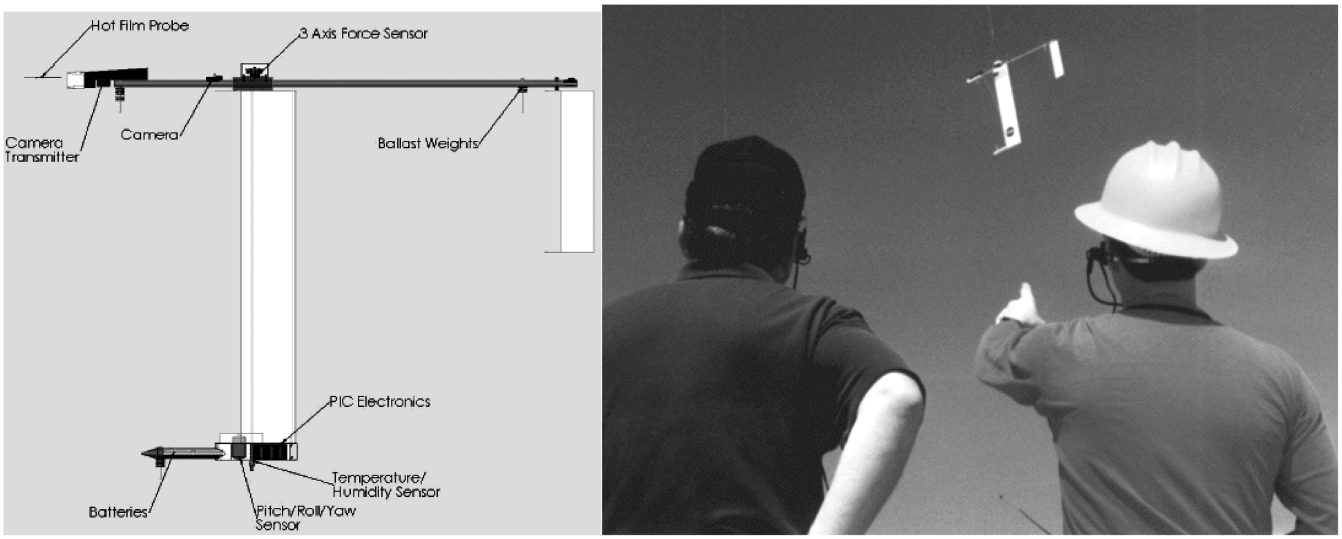

Fig. 5 Scale-model BGS.

does contribute to lift. Just based on the relative locations of the quarter-chord points of the main wing and rudder with respect to the c.g. of the system, the increased lift of the rudder could contribute as much as 7 to 10% (depending on the system c.g. location) to the total lift of the system. Thus, if the main airfoil lift coefficient was 0.90, the total lift of the system could be as much as 1.0. This number excludes any contributions of the boom. Of course, 3D effects will tend to lower the lift of the main wing. A full-scale flight test is really required to assess actual performance.

Even if turbulence during the scale-model test had inflated the lift performance of the system, a method of recovering that performance is available to us by introduction of roughness near the leading edge of the full-scale wing to recover the higher lift coefficient, as will be discussed in the next section.

C. Lift Enhancements

After the results of a full-scale flight test are known, there are several ways to enhance the lift of the BGS, if needed. We discuss some of these methods in three categories: simple surface modifications, increased wing surface area, and airfoil shape modifications.

1. Simple Surface Modification

It is well-documented that placing roughness on the suction surface toward the leading edge of an airfoil can increase the maximum lift coefficient at relatively low Reynolds numbers. For example, in experimental testing of small airfoil models, trip wires or sandpaper are often used to simulate higher Reynolds numbers than are achievable in some wind tunnels. Creating roughness is often achieved by gluing a strip of sandpaper along the span of the wing. This disturbs the boundary layer and causes turbulence, which allows the flow to remain attached to the surface beyond the point at which it would have otherwise separated. This effect mimics, to a certain extent, what occurs naturally at higher Reynolds numbers, for which the boundary layer becomes turbulent closer to the leading edge, and delays stall to higher angles of attack. If the freestream is turbulent (as

Table 2 Dynamic scaling of scale-model test

Important parameters	Full scale	Actual model	Units	Full/actual model
Scale	1	0.268		3.733
g	9.73	9.79	m/s^2	0.994
Altitude	20	0.9	km	22.222
Density	0.089	1.12	kg/m^3	0.079
Temperature	217	295	K	0.734
Dynamic viscosity	1.41E − 05	1.82E − 05	kg/m-s	0.776
Kinematic viscosity	1.59E − 04	1.63E − 05	m^2/s	9.773
Wingspan	5.5	1.41	m	3.902
Wingspan, ft	18.04	4.63	ft	3.902
Wingspan, in.	216.54	55.5	in.	3.572
Wing chord	1.1	0.308	m	13.935
Wing area	6.05	0.434	m^2	1.092
Aspect ratio	5	4.6		1.951
Froude number	9.343	4.789		2.632
Relative wind	10	3.8	m/s	0.962
Reynolds number	69,174	71,927		0.833
C_L	1.0	1.2		6.384
Lift force	26.90	4.21	N	26.757
Mass	90.00	3.36	kg	26.593
Weight	876	33	N	4.165
Weight/lift	32.6	7.8		1.000
C_{D_0}	0.02	0.02		0.675
C_D	0.126	0.187		5.169
Drag wing	3.39	0.66	N	5.169
Drag wing/lift	0.13	0.16		0.810
L/D	7.93	6.42		1.235
Time scale	0.110	0.081	s	1.357
Representative moment of inertia	226.9	0.56	$kg \cdot m^2$	407.292

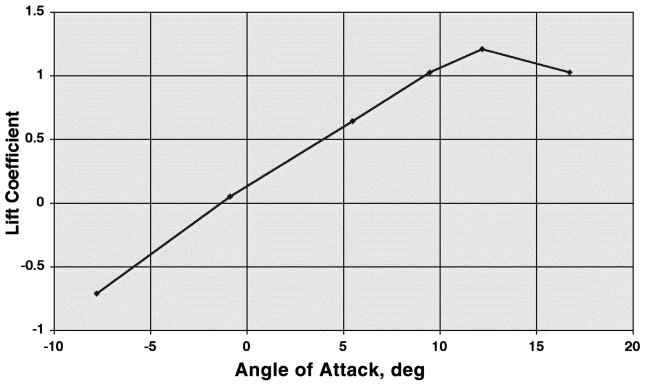

Fig. 6 Scale-model test lift coefficient versus AOA.

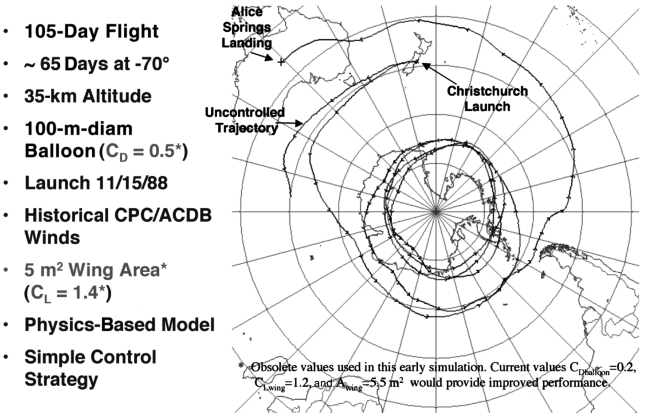

Fig. 7 New Zealand to Antarctica to Australia simulation.

in the case of our scale-model test), that also helps trigger the transition from laminar flow to turbulent flow within the boundary layer near the leading edge of the airfoil. Both surface roughness and freestream turbulence cause the boundary layer to act as though it were operating at a higher Reynolds number, all of which enhance lift in this range of Reynolds numbers.

Such surface features can be added to the BGS airfoil to keep the boundary layer attached longer as the AOA is increased, thus yielding higher lift performance. Some of these methods are extremely simple and inexpensive, if needed. Because they are so simple, it may be useful to consider including such surface modification on just one side of the wing for a full-scale flight test to determine its potential value (by comparing performance on opposite tacks).

2. Increased Wing Area

The current prototype wing assembly is estimated to weigh about 90 kg when fully instrumented. It was never designed to be terribly lightweight, due to the extreme budget limitations of the SBIR program. For an operational system, the current prototype wing assembly will probably require redesign, because it is unwieldy for routine launch operations. In such a redesign, the main wing could easily be increased in area by a factor of 2 without mass increase. Increasing the area of the main wing by a factor of 2 will increase BGS cross-track performance by approximately the square root of 2. We would not propose to increase the wing area until after a full-scale flight test of the current prototype system confirms that increased performance is necessary.

3. Airfoil Shape Modifications

A thicker airfoil and/or a trailing edge flap can significantly increase the lift of a symmetric airfoil. The flap feature essentially adds camber to the wing. If this flap is reversible, one can improve the lift performance of the wing in either direction of operation. There are concepts [15] for such relatively simple design changes that can improve on the lift performance of the NACA 0015 airfoil by about 100%. We would not recommend including a reversible flap, because of its obvious reliability and cost issues, unless a full-scale flight determined that such increased performance was really necessary.

V. Systems Performance

In this section, we discuss a particularly powerful example simulation of the performance of the BGS, the availability of differential winds, a random-walk illustration of the capability of underactuated systems, and a proposed method for determining BGS performance requirements.

A. Antarctica Simulation

In this section, we discuss an early Antarctica balloon simulation to demonstrate the BGS system performance.

1. Simulation Conditions and Assumptions

In 1999, we performed a computer simulation to illustrate the potential system performance of the BGS. Figure 7 illustrates this early simulation in which we transported the balloon from its New Zealand launch site to $-70°$ latitude for about 65 days then returned to a landing at Alice Springs, Australia, for a total mission duration of about 105 days. Each arrow on the path corresponds to one day of flight. This simulation used the CPC/ACDB[§§] wind data that are from the Climate Prediction Center analyses that are basically interpolations of satellite data (not assimilations).

One nice feature of this simulation is that it used a relatively high-fidelity physics-based model of the BGS operation. Later simulations have instead used simplified operations models to simulate performance and reduce run time. The key assumptions for this early high-fidelity simulation are listed on the left-hand side of the figure. Note that obsolete values for balloon drag coefficient (see the light-shaded text in Fig. 7), wing area, and wing lift coefficient were used in this early simulation. We still display this simulation to illustrate the performance of the balloon guidance system because more current values for these parameters would actually show improved performance (see the note at the bottom of Fig. 7). In fact, if we were to use a wing-assembly lift coefficient as low as only 0.5, the performance would be equal to that shown. One major change is in the assumed value for balloon drag coefficient. We are now using a value corresponding to the value it has after the balloon has accelerated past the drag crisis, in which the flow changes from laminar to turbulent, which produces a near-step-function reduction in the drag. When we created this early simulation, we were unaware that the balloon was near the drag-crisis regime. The key point is that the estimated cross-track performance of the mechanical prototype system we built is expected to be about 40% (the square root of 2) better than the system performance illustrated in this simulation using the same control algorithm, which can be improved upon.

The primitive control algorithm that was used for this simulation had the following characteristics. There was a $\pm 2°$ deadband and a larger $\pm 10°$ band around the desired latitude of $-70°$. Within the deadband, the control objective was simply a unit vector in the direction of current travel. Beyond the larger $10°$ band, the control objective was simply a unit vector to the north or the south. Between the proportional band and the deadband, the control objective was a unit vector in a direction between north (south) and the current direction of travel when the balloon was south (north) of the desired latitude. The control objective was determined by a linear combination of the north (south) vector and the direction of travel. Even with this crude algorithm, we were able to maintain the desired latitude range ($\pm 2°$) 55% of the time. Were the desired range

[§§]Wind data were courtesy of A. J. Miller of the Climate Prediction Center (CPC) at NCEP and P. A. Newman at the Atmospheric Chemistry and Dynamics Branch (ACDB) of the GSFC, who produced the winds. The GSFC Distributed Active Archive Center distributed this data as part of NASA's Mission to Planet Earth program.

expanded to ±5° from the desired latitude, the station-keeping percentage would become 88% of the time. And this is all with a system with about a factor of 40% less performance than we currently estimate is possible with our prototype system. In addition, with our experience over the last several years, we know that we could improve the algorithm significantly by doing the following:

1) Use a look-ahead strategy that would involve using forecasts of future winds. The objective is to get a good position three or five days hence, not worrying particularly about a problem on the next day. We have implemented these look-ahead capabilities on other simulations and they have been very successful.

2) Make the deadband narrower (0.5°) or eliminate it altogether.

3) Employ quadratic (or higher power) control schemes so that we get more control into the system when we are only slightly out of the deadband.

We could use these improvements separately or in combination to significantly improve performance.

2. Differential Winds in Simulation

Figure 8 presents the relative wind between the top and the bottom of the tether seen in the New Zealand to Antarctica scenario. In this figure, the winds are simply the scalar values: *Wind at balloon* is the magnitude of the wind speed at the balloon altitude without regard to the motion of the system. *Balloon velocity* is the speed of the balloon across the ground. *Wind at wing* is the magnitude of the wind speed at the wing altitude without regard to the motion of the system. Note that even when these two wind speed values are close, there could be large relative winds because of the vector directions. *Control velocity* is the true airspeed of the balloon; that is, the magnitude of its velocity with respect to the parcel of air in which it is moving. Control velocity is fully balanced, vectorially. This plot really does not give a good picture of the winds because it displays only the scalar magnitudes. One really has to look at the vector directions along with the aerodynamic model of the BGS to assess performance.

Figure 9 displays the relative velocity of the wind on the BGS wing that enables it to achieve the control velocity shown in Fig. 8. Given the vector wind differences, there is a variation in relative winds from a high of 33 m/s to a low of about 4 m/s (during the latitude station-keeping phase).

3. Simulation Control Authority

The next figure displays the cross-track and back-track velocities that result from the operation of the BGS. For this particular simulation, positive cross-track values (shaded for better visibility) generally correspond to northward nudging of the balloon and negative values correspond to southward nudging.

Very clearly, the relative winds shown in Fig. 9, combined with very conservative estimates of system aerodynamic performance that produced the cross-track velocities displayed in Fig. 10, enable the BGS to achieve a particularly striking scenario, which has a powerful impact on the discussion of potential mission opportunities enabled by balloon trajectory guidance/modification systems.

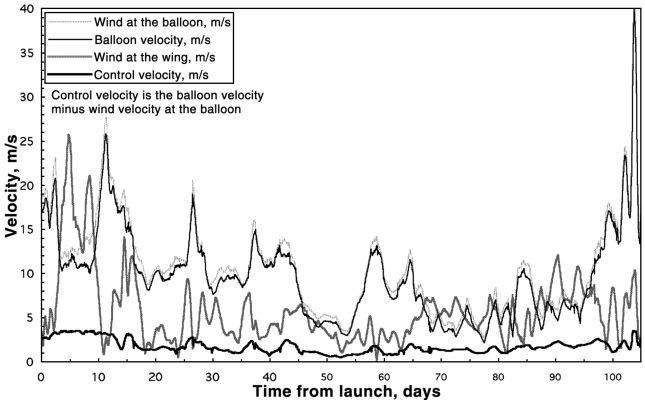

Fig. 8 Winds from New Zealand to Antarctica simulation.

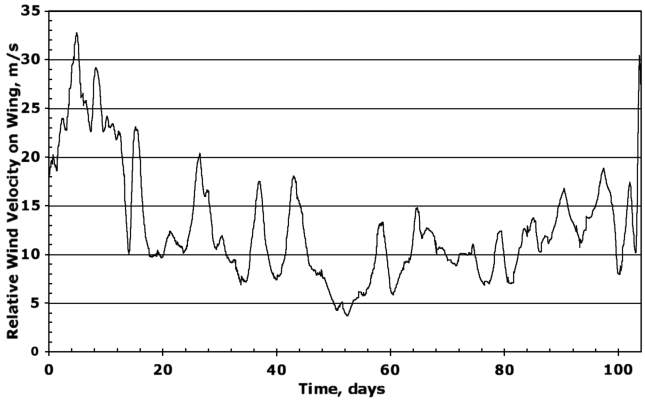

Fig. 9 Relative wind on the BGS wing for Antarctica simulation.

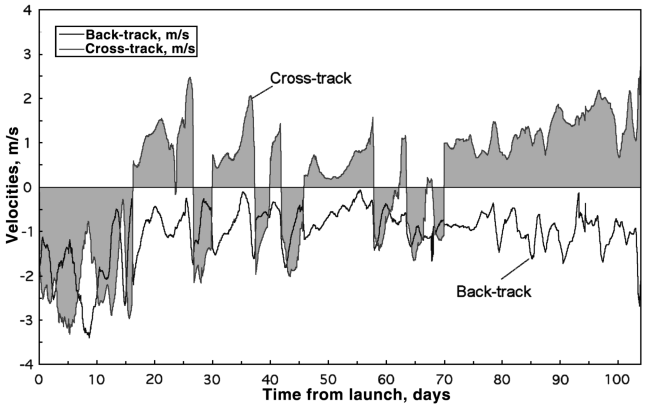

Fig. 10 Cross-track and back-track velocities of Antarctica simulation.

B. Performance Requirement

Early in our development of the BGS, we established a BGS performance design requirement of 1–2 m/s in the presence of a 10-m/s relative wind at the BGS wing. This requirement was levied on the design of the hardware, not on its operation. Unfortunately, this design requirement can and has been interpreted as an operations requirement. Such an operations requirement is, in fact, meaningless. No sailboat ever built could meet such an operations requirement solely using wind power, yet sailboats have provided useful motive power for millennia. More appropriately formulated operations requirements could be quantified using future analysis and simulations. An example of an appropriate operations requirement would be to require the system to maintain a specified latitudinal corridor during a specified period of time, such as December through February about the latitude of Alice Springs, Australia, for example. During our NASA-funded efforts, operations requirements were never analyzed or specified by NASA. In addition, GAC has not characterized the winged BGS envelope of operations, beyond the few simulations that we published. Even so, those simulations, including the one described previously, indicated the overall feasibility of the BGS for providing useful latitude control. In our opinion, the level of performance demonstrated by these conservative simulations is sufficient for the operation of the ULDB[¶¶] system, given its current technology goals and limited launch dates and sites. This assertion could be tested by more thorough analysis and simulations and by an actual flight test of the prototype hardware.

[¶¶]The ULDB is a superpressure balloon with fixed volume, for which the lifetime is primarily limited by gas leakage.

Table 3 Wind statistics for Alice Springs, Australia: December through April

Wind	Statistic	Dec.	Jan.	Feb.	Mar.	Apr.
Differential zonal wind, m/s	Mean	−13.7	−24.1	−24.8	−14.2	−0.1
	Std dev	9.7	8.6	8.6	9.4	9.9
Differential meridional wind, m/s	Mean	−0.3	−0.5	−0.5	−0.4	0.3
	Std dev	6.3	6.1	6.3	6.5	7.1
$P(\|ZW\| > 10$ m/s)		0.65	0.95	0.95	0.69	0.31
$P(\|V_{35}\|/\|ZW\| < 0.1)$		0.33	0.23	0.30	0.05	0.15

Table 4 Wind statistics for Antarctica: December through April

Wind	Statistic	Dec.	Jan.	Feb.	Mar.	Apr.
Differential zonal wind, m/s	Mean	−9.2	−6.3	−3.6	1.7	11.0
	Std dev	6.8	4.4	4.1	6.9	9.4
Differential meridional wind, m/s	Mean	0.1	0.4	0.5	−0.1	−0.4
	Std dev	6.4	4.1	4.5	6.8	9.3
$P(\|ZW\| > 10$ m/s)		0.44	0.18	0.06	0.15	0.54
$P(\|V_{35}\|/\|ZW\| < 0.1)$		0.16	0.17	0.09	0.19	0.15

Table 5 Wind statistics for Christchurch, New Zealand: December through April

Wind	Statistic	Dec.	Jan.	Feb.	Mar.	Apr.
Differential zonal wind, m/s	Mean	−29.5	−30.1	−21.0	−6.2	6.2
	Std dev	8.9	7.2	8.3	10.3	13.1
Differential meridional wind, m/s	Mean	-0.4	−0.2	−0.3	−0.2	−0.2
	Std dev	6.4	6.0	6.5	7.3	8.5
$P(\|ZW\| > 10$ m/s)		0.99	1.00	0.90	0.43	0.50
$P(\|V_{35}\|/\|ZW\| < 0.1)$		0.60	0.45	0.24	0.23	0.16

Table 6 Wind statistics for Kiruna, Sweden: May through August

Wind	Statistic	May	June	July	Aug.
Differential zonal wind, m/s	Mean	−9.6	−11.3	−10.5	−6.2
	Std dev	5.9	4.1	3.9	4.5
Differential meridional wind, m/s	Mean	0.2	0.1	0.1	0.0
	Std dev	5.3	3.7	3.6	4.3
$P(\|ZW\| > 10$ m/s)		0.48	0.62	0.54	0.20
$P(\|V_{35}\|/\|ZW\| < 0.1)$		0.21	0.34	0.21	0.23

C. Value of Wind Statistics in Measuring Performance

In this section, we discuss a BGS performance relative to wind statistics and how statistics can be used to assess performance and how statistics can be misused, if used alone in absence of other analysis techniques.

GAC has studied wind statistics for the range of potential ULDB launch sites and seasons using the NCAR Reanalysis 2 data.*** Tables 3–6 summarize the wind statistics calculated by GAC for four typical balloon launch sites (±2.5° latitude) and seasons for 10 years of wind data using the NCAR data set. We take note of the probability of experiencing a zonal wind difference greater than 10 m/s, $P(|ZW| > 10$ m/s). This probability is very favorable for Alice Springs, Australia and Christchurch, New Zealand for several months; however, it is rather low for Kiruna, Sweden and even lower for McMurdo Station, Antarctica. In particular, we note the low probability of having a zonal wind difference greater than 10 m/s (i.e., about 0.18 for January in Antarctica for the selected latitude band). This is a low probability that could place into serious question the viability of the BGS to achieve meaningful control given these mean conditions. First, one needs to ask whether such wind statistics can be useful in determining the performance of a BGS.

Because our Antarctica simulation used winds from November 1988 through February 1989, we focused on looking at wind statistics for this time frame. To study this question, we generated wind statistics, including the probability of having a relative wind sufficient to counteract the meridional drift at 35-km altitude for January 1989 for the simulation seen in Fig. 7, using the NCAR and CPC data with varying latitude zones. Table 7 summarizes and compares these data.

We find that the mean zonal wind differences are generally higher for the simulation wind data (note the different dates and latitudes) and the standard deviation for the meridional winds at 35-km altitude are generally lower. These differences map into an overall probability of having a relative wind greater than 10 m/s of 29% for the simulation, depending on the time span assumed. We also calculated the probability of having a zonal wind difference sufficient at any particular time to counteract the meridional drift. In addition, to do a fair comparison between the wind statistics from the simulation with that expected over a zone, we developed statistics for a latitude band that encompasses the simulation latitudes and different-sized zones centered on the launch site latitude. We thought that the wider band of operation for the simulation (±4.7° vs ±2.5°) may contribute to a reduction in meridional winds standard

***Data available online at http://www.cdc.noaa.gov/ [retrieved 2_May 2007].

Table 7 Antarctica wind statistics comparison

Wind	Statistic	January NCAR Re2 data, 10/92–9/01	January NCAR Re2 data, 10/92–9/01	GAC sim January 1989 CPC[a]	January 1989 CPC	January 1989 CPC
Latitude band		78°S ± 2.5	78°S ± 4.7	71.8°S ± 4.7	71.8°S ± 4.7	78°S ± 2.5
Differential zonal wind, m/s	Mean	6.3	6.2	8.4	8.5	4.3
	Std dev	4.4	5.3	2.7	3.6	1.8
Differential meridional wind, m/s	Mean	0.4	0.3	−0.6	0.0	0.0
	Std dev	4.1	4.1	1.5	1.8	1.4
Meridional wind at 35 km, m/s	Mean	0.3	0.3	0.1	0.0	0.0
	Std dev	3.4	3.4	1.3	1.4	1.4
$P(\|ZW\| > 10$ m/s)		0.18	0.22	0.29	0.33	0.00
$P(\|V_{35}\|/\|ZW\| < 0.1)$		0.17	0.20	0.48	0.45	0.25
BGS control velocity, m/s	Mean		0.67	0.77	0.85	0.43

[a]One-hour data only along the flight path. Interpolated CPC data for the period of the simulation shown.

deviation. To test this hypothesis, we ran 10-year wind statistics over a wider latitudinal band.

For the data in Table 7, all the probabilities of achieving a greater than 10-m/s zonal wind difference appear low, yet our simulation illustrates the ability of the BGS to effectively control the balloon trajectory; that is, *a reduced-performance BGS*[†††]*can effectively control the latitude of balloon operations*. The message is that wind statistics alone cannot tell the story of the ability of the BGS to control latitude. We speculate that one reason for this is due to the fact that the balloon is in a pseudo-Lagrangian reference frame (moving with the flow), not an Eulerian reference frame (fixed in space).

By comparing wind analysis along a trajectory for January 1989 with the wind analysis of the wind field within the latitudinal band 71.8° ± 4.7°, we can see that they give similar values for wind statistics and probabilities of achieving a greater than 10-m/s zonal wind difference. Hence, analysis of the wind velocity and direction distributions in a wide latitudinal band can be used as a proxy for similar analyses along a flight path in that latitude band. We see that the probability of achieving a greater than 10-m/s zonal wind difference for the band encompassing our simulation was just about 30%. However, from the actual simulated trajectory, we know that it was well-controlled: we steered the balloon roughly where we wanted it. Hence, a probability of 30% is sufficient to control the trajectory. We cannot say, without further analysis, how small this probability is before there is insufficient control. The bottom line is that a simulated controlled balloon trajectory gives the ultimate answer about utility and performance of a BGS. The wind analysis and comparison with the simulated trajectory tells us that the probability of 30% of exceeding a 10-m/s zonal wind difference represents favorable conditions for trajectory control. There is another perspective, as alluded to earlier, from which to view this issue: namely, the differences between Lagrangian and Eulerian reference frames, which will be discussed next.

In fluid dynamics, the Lagrangian reference frame is a way of looking at fluid motion in which the observer (the balloon) follows individual fluid particles (the atmosphere) as they move through space and time. But, in the case of the balloon, it generally stays at a fixed altitude; hence, it is in a pseudo-Lagrangian frame of reference. The Eulerian reference frame is a way of looking at fluid motion (the atmosphere) that focuses on specific points (or grid points) in the space through which the fluid moves. The wind statistics are the result of an Eulerian analysis whereby the wind data are calculated at particular gridded data points. Yet the balloon floats with the wind in a pseudo-Lagrangian reference frame. It would not be surprising that the BGS performance determined from these two frames of reference would be different. The reason they would be different is that the balloon winds are highly correlated hour to hour and day to day; that is, if the balloon is drifting north today, tomorrow it is likely to be still drifting north. The wind statistics of a latitude band, or even from an entire simulation, can have relatively large standard deviations, yet the actual winds felt at the balloon are very correlated. Meridional winds that we calculated show large variability. Winds with such variability could send the balloon to the equator in a few weeks, yet in reality this almost never happens in real simulations. If one studies the ULDB Antarctica mission analysis we carried out for NASA,[‡‡‡] one can see that with very few exceptions, even unguided balloons in December and January do not move far northward from the launch latitude in Antarctica, even over a 120-day period.

D. Random-Walk Illustration

It may not be obvious that a small level of control authority should be able to overcome fairly large variances in winds. To clarify this aspect of balloon trajectory guidance, we created a much simpler MS Excel simulation of a random walk, with a small amount of control that would be relatively easy for someone else to duplicate so that they could see for themselves how effective even a small amount of control can be in the presence of disturbances with a fairly large variance.

The model simulates a random walk in which a disturbance velocity (somewhat analogous to the cross-track wind at the balloon) is represented by a random variable following a normal distribution and a deterministic control value. The normal distribution is characterized by a mean value and standard deviation selected by the user. In the absence of any control, the random walker would simply move at the velocity of the random disturbance over one time step. Figures 11a–11d illustrate paths followed by ten different random walkers for 1000 time steps for cases in which the mean of the disturbance velocity is 0 or 0.2 and the standard deviation of the disturbance velocity is 3.0, and for cases in which control is either 0 or 0.5. The horizontal axis could be thought of as time, with the vertical axis as the distance the random walker has moved from the starting point. Each of the plotted zigzaggy lines could be thought of as the path followed by a different random walker released at time zero. The various parameters are dimensionless. The two solid curves represent the predicted two-sigma envelope of the simulated trajectories from classical theory.

As expected, the simulated trajectories are mostly bounded by these two curves, but extend beyond them a small fraction of the time: about 5% of the time (according to theory, we would expect to find a random walker in a normal random field outside the two-sigma bounds 5% of the time). Also, as predicted by theory, the random walks diverge from zero with a dependence that is proportional to the square root of time. The equation for the two solid curves is simply two (for two sigma) times the standard deviation (sigma) of the disturbance velocity times the square root of time.

The first case, Fig. 11a, illustrates paths followed by ten different random walkers for 1000 time steps when the mean of the disturbance velocity is zero and its standard deviation is 3. If we add a mean value to the disturbance velocity, as in Fig. 11b, then a general drift is superimposed on the random motion. Here, the value of the

[†††]Remember, the system performance of the BGS in the Antarctica simulation was about a factor of 40% lower in performance than we now expect of the system we designed and built, as discussed in Sec. II.

[‡‡‡]"Ultra Long Duration Balloon (ULDB) Antarctica Mission Analysis: Final Report," Global Aerospace Corp., Rept. 191-59585-002, Altadena, CA, May 2003.

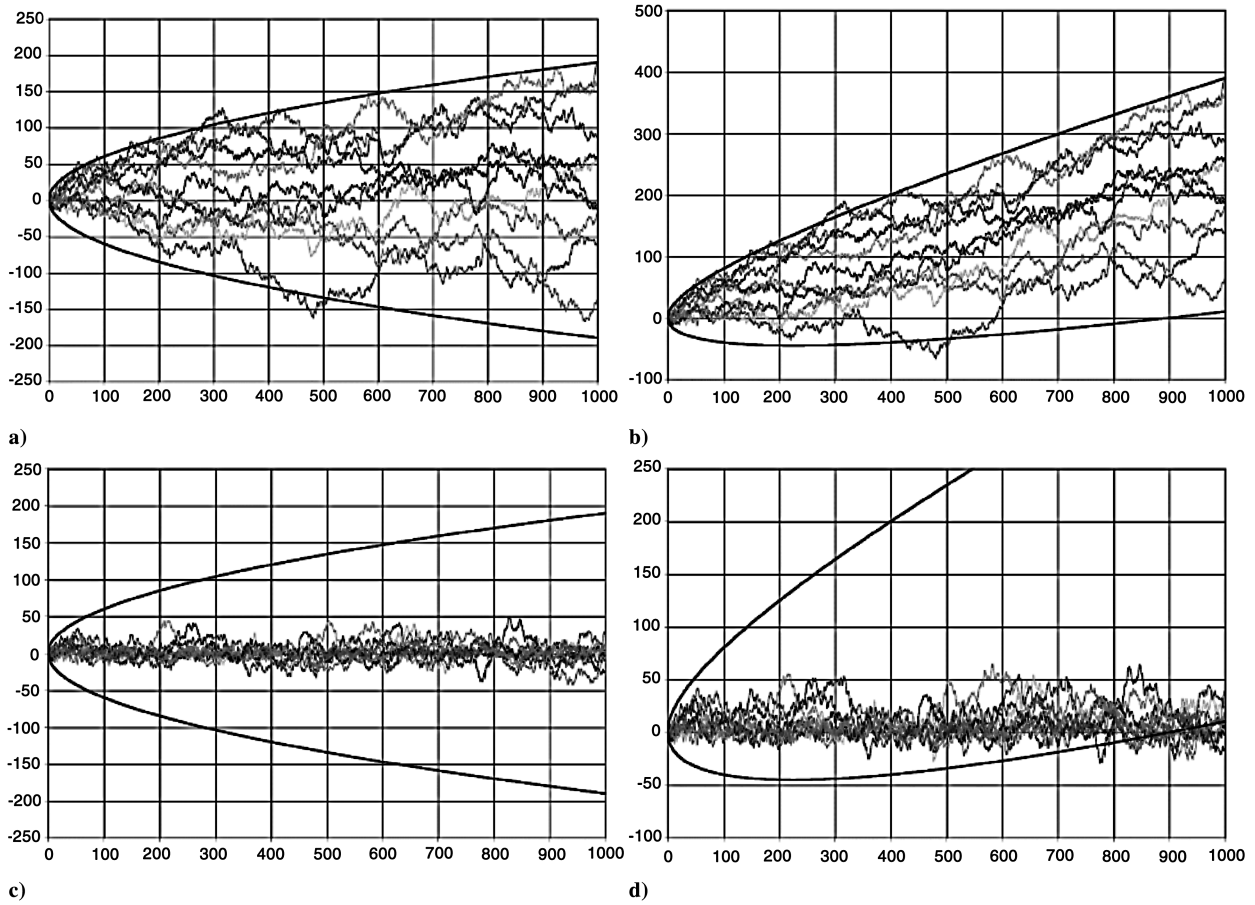

Fig. 11 Random-walk illustration in which a) the mean of the disturbance velocity is zero and its standard deviation is 3; b) the mean of the disturbance velocity is 0.2 and its standard deviation is 3; c) the mean of the disturbance velocity is zero, its standard deviation is 3, and the control is 0.5; and d) the mean of the disturbance velocity is 0.2, its standard deviation is 3, and the control is 0.5.

mean of the disturbance velocity is set to 0.2, and so after 1000 time steps, there is a systematic motion of 200 steps added to the random motion. For all these simulations, we used the same ten sets of 1000 random variables rather than creating new values each time. Going back to the first case, with zero mean and a standard deviation of 3, we turn on a control velocity capability of 0.5 and get the behavior shown in Fig. 11c. Here, we left the original solid two-sigma lines for reference. At each time step, we simply added a control velocity equal to 0.5 directed toward the origin. That is, if the displacement is positive, we add -0.5 to the disturbance velocity, and if the displacement is negative, we add $+0.5$ to the disturbance velocity before calculating how far the walker would move during that time step. It can be seen that a relatively small amount of control is remarkably effective at overcoming the random disturbances. Now consider a final illustration, Fig. 11d, in which the same level of control (0.5) is applied to the case with a disturbance drift velocity of 0.2 (note that the two black curves represent calculated two-sigma trajectory bounds *without* added control velocity).

The figures demonstrate that *a relatively small amount of control is quite effective* at overcoming random disturbance velocities in addition to fighting a systematic bias. Naturally, the control velocity must be greater than the mean bias velocity or else the system will be blown further and further off course. As we have seen in the discussion on wind statistics, this is indeed the case in a real atmosphere in the several analyzed cases, in which the mean meridional velocity in a narrow latitudinal corridor (typically, 0.0 to 0.3 m/s) is smaller than the mean control velocity generated by the BGS (typically, greater than 0.5 m/s).

E. How to Characterize BGS Performance

We believe that wind statistics can be useful once detailed studies have been carried out so that one can understand what the wind statistics mean. However, wind statistics alone cannot be used to determine the performance capability of a winged BGS. It is more important that the BGS be able, on average, to control the latitude of the balloon to some acceptable tolerance. A better way to determine this performance capability is to run many simulations over a span of several years' worth of wind data and to characterize the statistics of its control capability as a function of launch site, season, latitude tolerance, wing aerodynamic performance, etc., and then assess the resulting control performance statistics. One may also want to parameterize control objectives in these studies to understand what should be the operations requirements for a given BGS design. It is not important that the zonal wind difference is less than 10 m/s, but rather, whether the existing wind difference combined with aerodynamic performance of the BGS is sufficient to counter the average meridional drift.

VI. Concept of Operations

In this section, we discuss the system concept of operations for an operational BGS on a balloon. We make the distinction between an operational system versus an earlier flight demonstration of a prototype BGS, such as the mechanical prototype that we built. For the purposes of this discussion, we assume that the ULDB is at a fixed-density altitude of around 35 km and the BGS wing assembly is at a 20-km altitude.

A. System Characteristics

An operational system is expected to be lightweight compared with the total suspended mass carried by the balloon. Our current best estimate of the total mass of the flight demonstration prototype BGS, with a very conservative contingency, is about 155 kg or about 5% of the suspended mass of the ULDB. Most of this mass, about 90 kg, is

the BGS wing that is suspended below the gondola. At this point, we have no reason to believe an operational BGS to be different in mass from the prototype BGS. The operational BGS could be lighter or heavier, depending on the level of technology incorporated, the design approach used, and the system and performance requirements imposed.

The BGS wing assembly includes a controller, mechanical devices for deployment and termination, rudder and rudder actuator, a small self-contained power system, and flight and engineering sensors. The prototype system fixed wing is 5.5 m long and has a wing chord of about 1.1 m. The main wing and the rudder are mounted on a 4.9-m-long boom. The operational system could have different dimensions, depending on requirements. To facilitate launch operations, we envision the operational wing assembly to be compactly stowed below the gondola in a small package, unlike the flight demonstration prototype. Several stowage options exist that use a variety of state-of-the-art design and fabrication techniques, including inflatable and collapsible structures.

The BGS interface package, estimated to be about 65 kg, is located on the gondola and consists of a winch, controller, radios, flight and engineering sensors, mechanical devices for deployment and termination, and power interfaces with the gondola. A major innovation of the Global Aerospace Corporation winged BGS is in the design of the tensioning system that allows us to use commercial tether spools, thus reducing tether-spool mass from 180 kg on the Harvard reel-down experiment [16,17] to about 3–6 kg for the BGS interface package. The Harvard system was almost the entire balloon payload at nearly 1500 kg and was quite different from the Global Aerospace Corporation BGS because it was a cost-constrained, single-flight system designed for high-speed reeling (up and down) and it had a self-contained power system.

The tether is braided cable nominally made from polybenzoxazole (PBO) fiber. We estimate that the mass of the tether, including its UV/light protection, will be about 1–2 kg/km of tether length, depending on the mass of the operational BGS and the required safety factor on the tether.

B. Deployment

BGS wing-assembly deployment is expected to occur in two phases. Soon after launch, the BGS wing assembly is released from its restraints and expanded or unfolded to its full size below the gondola. This initial deployment occurs early during the ascent, when environmental conditions are still benign. The operational BGS remains in this state, still partially restrained, until the balloon reaches its float altitude of 35 km. Upon reaching float and determining that the mission is a "go," the BGS wing is then lowered 15 km to its operational altitude of about 20 km. This winch-down procedure could take several hours, depending on operational considerations. Because balloons are often launched in the early morning after several hours of preparation, there is a desire to complete any mission critical event, such as BGS deployment, that same day. The faster the winch-down process, the more energy that must be dissipated. The rate of energy dissipation affects that system mass and complexity, thus a design trade-off will eventually need to be studied. Current assumptions are that the BGS will be fully deployed at its operational altitude 8–18 h after reaching float or about 10–20 h after launch.

C. System Control

As with an elevator of an airplane, the rudder position on the BGS wing assembly will determine the angle of attack of the relative wind on the main wing and thus the direction and magnitude of lift on the system. An actuator affixed to the boom will rotate the rudder into the desired position. The BGS wing assembly will be controlled and monitored via a radio link between the BGS interface package on the gondola and the wing at 20-km altitude. The balloon gondola, in turn, is monitored from the ground via a satellite communications relay link. Both the BGS wing assembly and the BGS interface package on the balloon gondola will be instrumented with flight sensors that will provide information on the balloon and BGS states and environments, including relative wind speed and direction. These data, combined with environment data assimilations and forecasts, will enable balloon ground controllers and navigators to make decisions on the BGS control actions that will influence the balloon path. It is expected that these decisions and actions will occur on a daily basis rather than in real time, because the winds aloft change very slowly and the balloon ground speed is relatively slow (e.g., only 10–30 m/s) during favorable seasons of operation for the ULDB.

The BGS can be used even without the availability of forecast wind information, provided real-time wind information is available either at the balloon from in situ measurements or data assimilations. In our early studies, we conducted a simulation that assumed the availability of a five-day forecast. We concluded that accurate five-day look-ahead trajectories are sufficient to provide time for a 2-m/s trajectory control to avoid a region (avoidance zones near cities) of this size (4 by 4°). However, we never concluded that five-day forecasts are required for BGS operation. We believe that in many cases for ULDB operations, wind forecasts are not required to operate the system. Without forecasts, operators will steer further away from exclusion zones. However, if forecasts are available, much more efficient operations can be mounted.

D. Flight Termination

There are two flight termination cases that we considered. The first case is nominal planned mission termination in which the gondola is cut away from the balloon and allowed to fall to the Earth via a parachute and in which the balloon envelope is ripped open to release helium and allowed to fall to the ground. In this nominal case, the BGS tether is severed before separating the gondola from the balloon. The tether is severed at both ends nearly simultaneously to reduce horizontal tether drift due to winds aloft. The BGS tether then falls to the ground in the same way as the balloon envelope. At this point, we are assuming that the tether clumps on its way to the ground, as discussed later. After the BGS wing assembly is cut away from the tether, it falls to the ground via a small parachute. Depending on system requirements, much of the high-value BGS wing-assembly hardware, electronics in particular, could be refurbished for reflight.

There have been safety concerns raised in the past with the implications of cutting away a 15-km-long tether. It has been our assumption from the beginning of BGS development that if the 15–30-kg tether ends up in a compact clump on the ground, it would present considerably less danger to people and property than the 2200-kg ULDB balloon envelope descending to the ground. On the other hand, it could end up widely distributed on the ground due to winds aloft. If this were to happen, the tether could become a safety hazard to personnel (e.g., on open vehicles) and property (e.g., power transmission lines) on the ground. Over the ocean, these issues should not be a concern because the tether is expected to be denser than saltwater, hence it will sink to the bottom.

There is a physical argument why the tether will clump. Higher aerodynamic drag on the lower portion of the free tether (at 20-km altitude) is expected to cause it to fall more slowly than the top of the tether (at 35-km altitude), thereby causing the tether to collect at the bottom during descent. If this understanding of the physics is correct, cutting the tether before flight termination would result in a compact tether on the ground, thus the fallen tether would not present a safety concern. Without safety concerns, tether reel-up is not necessary. There was a single tether drop test carried out by NASA in the early 1980s under the Harvard reel-down experiment [16,17]. A 20-km tether was deployed and then cut away from a balloon. Unfortunately, the tether was never found. This is either because the tether never deployed properly and was dropped as a single package or that it fell into a single clump that was difficult to find. Any future tether drop test must determine the state of the tether before, during, and after the drop. In addition, the tether must be able to be located after it reaches the ground. A feature to be included at one or both ends of the tether is a small beacon, similar to those used to track small animals, to facilitate locating the tether after it reaches

the ground. If, in future flight tests and tether dynamics model runs, the tether does not clump reliably, we will need to reel the tether up to the gondola before separating the gondola from the balloon.

In the case of emergency termination, which can occur automatically when the balloon envelope ruptures catastrophically, the tether is cut at both ends just before cutting the gondola from the balloon. In this case, even if the tether does not usually clump, it is not reeled back up the gondola because there is not enough time before the gondola needs to be cut away from the balloon.

VII. Near-Space Applications

Potential mission applications of a winged BGS are in guiding scientific, communications, and national defense near-space balloons.

A. Scientific Balloons

The winged BGS was originally conceived by Global Aerospace Corporation to guide NASA ULDBs. However, since its conception, we have explored several other scientific balloon applications for guiding single balloons and regional and global networks of balloons.

Free balloons carrying science instruments typically drift freely in the prevailing wind at the operating altitude. In many cases, launch of such balloons must be delayed until forecast winds are projected to carry the balloon system into a region of interest or away from a forbidden zone. Frequently, such balloon flights must be terminated prematurely to avoid flying over countries that have not given overflight permission, to ensure that the payload descends into an appropriate landing site, or to avoid endangering densely populated regions. ULDB platforms will be no different, however, because they fly considerably longer than zero-pressure balloons[§§§] and prevailing winds can take them very far from their launch latitude. The ability to provide even a small amount of trajectory control could eliminate these reasons to terminate the flight early. Such an approach to balloon guidance 1) offers increased balloon operations flexibility and cost reduction, 2) permits the balloon to remain at a fixed-density altitude, 3) avoids overflight of uncooperative countries, 4) increases the number of potential landing sites, 5) enables the balloon to travel over desired locations, 6) passively exploits natural wind conditions, 7) does not require consumables, 8) avoids payload disturbances caused by propulsive trajectory control methods, 9) requires very little electrical power, 10) operates day and night, 11) offers a wide range of control directions regardless of wind conditions, and 12) can be made of lightweight materials.

A winged BGS could be used on long-duration balloons (LDBs) in Antarctica or in the Arctic. In Antarctica, it could help ensure that balloons stay over the continent and close to the pole, to minimize solar array power supply variations and to minimize diurnal altitude variations, and it could also deliver the payload back to a location near McMurdo Station, from which the entire payload could be recovered for future reflight, not just the chunks that fit through the door of the Twin Otter recovery aircraft, if one is available. Sixty-day flights could become routine. In summary, the BGS is important to extended-duration balloon programs because it simplifies mission operations by mitigating overflight and safety concerns, expands flight termination options, and minimizes payload recovery logistics.

Global Aerospace Corporation has also been funded by NASA to study the use of this technology for guiding balloons dedicated to Earth science [18,19]. These studies have demonstrated the capability of advanced BGS designs for guiding regional and global networks of balloons. Guided stratospheric balloon platforms, moved around the globe by the prevailing zonal stratospheric winds, have a multitude of Earth science applications, such as measuring profiles of concentrations of ozone and trace constituents, monitoring Earth magnetic field and radiative fluxes, tracking hurricanes, and monitoring global weather and climate. Networks of these guided balloon platforms can be configured to provide independent observations and to validate observations of other ground and space-based sensors. These platforms use a small amount of trajectory control to meet observation objectives. This guidance capability allows for rapid adaptation of network configuration to observational needs. In one NASA-funded study, scientists identified[¶¶¶] the applications of such stratospheric platforms to carry out Earth science goals, as described next.

There are several potential geomagnetic applications of guided stratospheric platforms. They can be used to study the nature of the middle and lower crust, to monitor the South Atlantic magnetic anomaly, to study the subice circulation in polar regions, to detect natural hazards through their associated magnetic signatures, and to study stratospheric/atmospheric processes with magnetic signatures. Guided stratospheric platforms allow a number of advantages over current platforms (satellites, aircraft, and surface stations) used in geomagnetic surveys, such as the ability to reliably separate the internal and external components of the Earth's magnetic field by measuring vertical filed gradients, to access hard-to-reach sites, to add intermediate spatial wavelength components to the existing surveys, and to warn spacecraft about space weather events.

Scientists have identified the verification of satellite measurements by direct measurements of Earth radiation budget (ERB) fluxes from the top of atmosphere (TOA) as the main application for guided stratospheric platforms. These measurements include broadband and spectral angular measurements of ERB fluxes, simultaneous determination of atmospheric parameters (pressure, temperature, and humidity), and cloud and atmospheric aerosol parameters. One of the major advantages of stratospheric platforms for ERB measurements is the direct measurement of the ERB fluxes that does not require radiance-to-flux conversion (satellites only measure radiance). Other advantages of ERB observations from stratospheric platforms versus satellites are the ability to observe flux dynamics on temporal scales that are not available from satellites, the capability of relatively large payloads (compared with satellites), and the related ability to make simultaneous in situ and remote measurements with different instruments.

Scientists have also identified several potential atmospheric applications of guided stratospheric balloon platforms. Guided stratospheric platforms can be used to monitor the water content of the stratosphere and study the processes that may be changing it, to monitor and study the decrease of ozone content in the lower stratosphere in northern midlatitudes, and to study the budget of greenhouse gases in the atmosphere. The advantage of being closer to Earth than space satellites may allow reducing the size and cost of light detecting and ranging (LIDAR) sensors and placing them on stratospheric platforms for atmospheric wind measurements. Such measurements may improve the ability to forecast hurricane paths. Other advantages offered by guided stratospheric balloon platforms include high-resolution in situ measurements, in situ validation of satellite measurements, higher resolution and higher signal-to-noise ratio of remote sensing instruments, and the ability to provide a snapshot of evolving stratospheric trace-gas structure.

B. Communications Constellations

As with guided Earth science balloons, an advanced BGS can guide constellations of stratospheric balloon communications platforms for providing cost-effective communications in rural areas, in which the cost of telephone or cellular infrastructure is not worth the investment, or in locations in which a disaster has disrupted conventional communications systems. Imagine a person working on an oil rig in the middle of the Gulf of Mexico. If they want to call home, they must use a $600–1000 satellite phone and pay $50 per month and up to $6 per minute of call. But what if they could use a

[§§§]Zero-pressure balloons are open at the bottom, to allow buoyant gas to escape and to reduce stress on the thin envelope, typically polyethylene, and thus their volume is determined by the temperature of the lifting gas. In diurnal conditions, their life is limited to only a few days by available lifting gas and ballast.

[¶¶¶]Data available online at http://www.gaerospace.com/projects/Strato-Balloons/pdfs_dosc/ESTO_GSB_SWG_ReportAv2.pdf, [retrieved 2 May 2007].

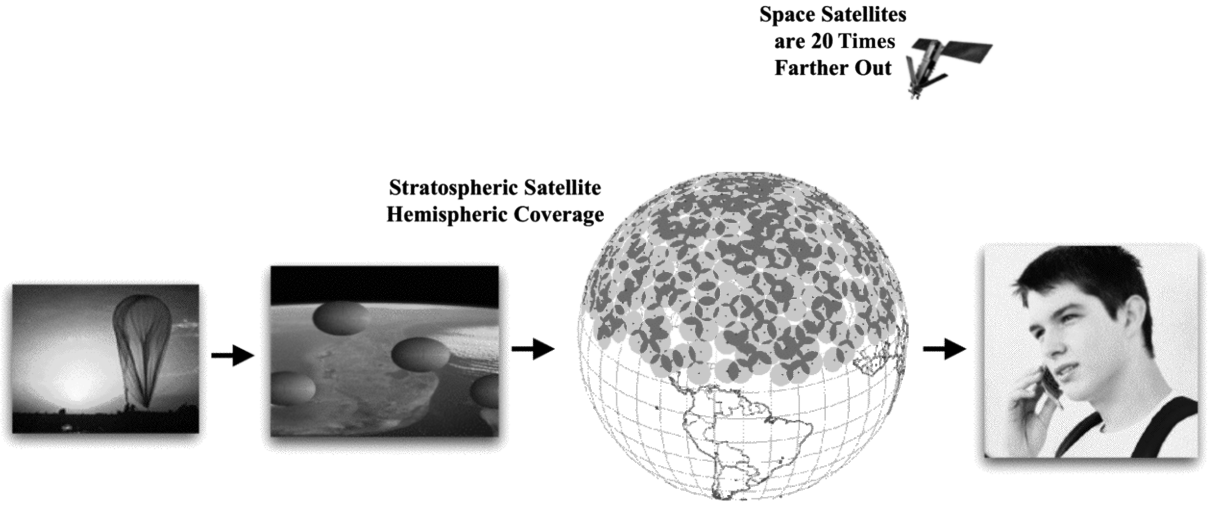

Fig. 12 Communications from guided constellation of stratospheric balloons.

regular cell phone without being charged expensive service fees? Guided stratospheric balloon platforms could provide the first truly remote cell phone service anywhere on the planet: over water, in mountainous terrain, in remote forests, and in deserts. Such stratospheric satellites would be steerable and would carry communications equipment above commercial airspace. Figure 12 illustrates a northern hemisphere communications network concept. In the constellation illustration, balloons are at the center of the lightly shaded circles that represent balloon coverage zones. The darkly shaded zones represent coverage overlaps between balloon platforms.

These floating constellations could act like "floating cell towers" that could bring low-cost cellular service to the maritime industry and other remote parts of the world for the first time. They would be low-cost because they would not require the enormous launch and hardware investment of space satellites, nor would they require a large hardware and labor infrastructure required of short-life, disposable, balloon platforms. GAC has studied the use of advanced versions of the BGS for guiding these stratospheric satellites. We found that a 400-platform network, which could cover 95% of the northern hemisphere, could be put into place for roughly the same order of magnitude cost of deploying a typical space satellite.

C. National Defense Networks

Historically, space surveillance and missile-detection missions have been considered to be applications of space satellite technology. However, space satellites and their sensors are expensive because their launch costs are very high. High launch costs necessitate high reliability with block and functional subsystem redundancy because they cannot easily be returned for repair, they require radiation-resistant electronic parts and optics because they fly in a space radiation environment, and they have complex and redundant computers and elaborate software designs to respond to subsystem failures. In addition, space satellites are increasingly viewed as vulnerable to attack by relatively inexpensive antisatellite weapons.

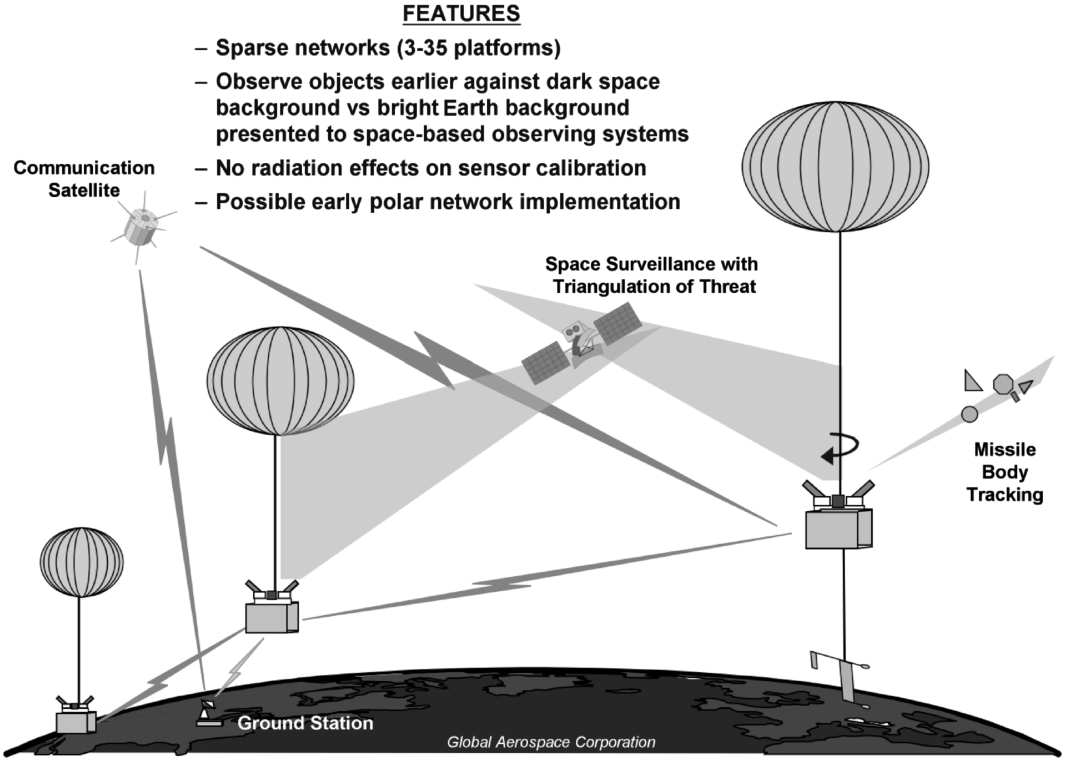

Fig. 13 Concept for stratospheric balloon constellations for space surveillance.

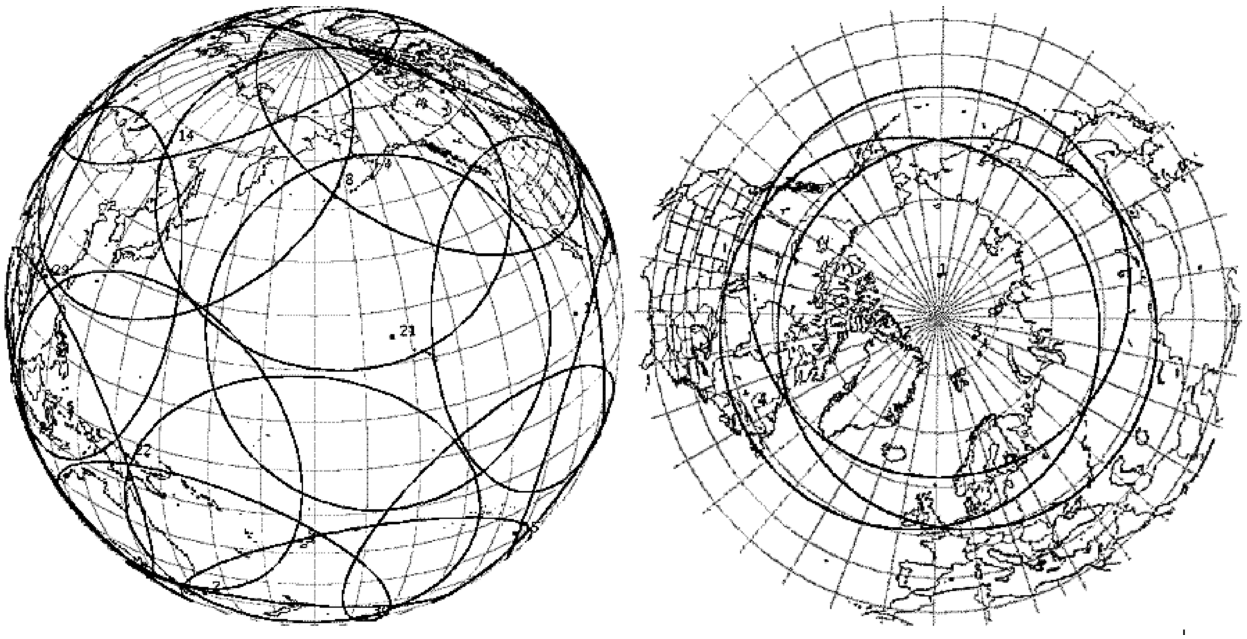

Fig. 14 Notional space surveillance balloon networks (global on the left and polar on the right).

The high cost of major satellite systems, and this increasing vulnerability, has prompted the examination of alternative means of meeting these important requirements. Figure 13 illustrates one space tracking and surveillance concept using low-cost guided-balloon platforms. GAC has studied the vulnerability of such systems to attack and have concluded that although systems can be developed to attack such stratospheric platforms, none exist today, and were they to be developed, the cost of deploying them would be costly relative to the cost of the platform and ease of its replacement, which is a very different situation from that for space satellites.

Figure 14 illustrates a polar network of three balloons (on the right) that could be deployed relatively quickly over the poles to search for high-inclination space targets and a global international space surveillance network (on the left) that could be distributed globally to search for all space targets. Here, the coverage circles illustrate the region around the balloon in which space targets could be seen by platform sensors when a target is above 1000-km altitude (along a line of sight that has a minimum altitude of 10 km). An international global network is estimated to cost less than $200 million to deploy versus the $10–23 billion that the U.S. Congressional Budget Office estimates a space-based surveillance system will cost to deploy.

VIII. Conclusions

We summarized the current development status, the physics of operation, the aerodynamic and systems performance, a concept of operations, and potential applications of our passive winged BGS. In particular, our research has confirmed that its aerodynamic performance, combined with available differential winds, provides a very significant balloon guidance capability for future very-long-duration, high-altitude, scientific balloons. This work confirms that a winged BGS provides the best and most efficient technology known to be available for guiding high-altitude balloons, based on data from prototype test flights and experimental data. Finally, we briefly explored applications for balloon guidance systems in scientific, communications, and national defense arenas.

Acknowledgments

We acknowledgment the support and encouragement of Jack Tueller and Warren Wiscombe at NASA Goddard Space Flight Center (GSFC) and the late Chuck Williams at NASA Wallops Flight Facility (WFF). In addition, we thank members of the StratoSail® balloon guidance system engineering team and its subcontractors over the years, including Keith Baker, J. Balaram, Nathan Barnes, Doug Bentley (Cortland Cable Company), Dale Burger, Jeff Gensler, Nate Hazen (consultant), Shannon Jackson, Dave McGee, Susan Nock, R. Stephen Schlaifer, Rich Trickel and the late Vance Jaqua (CI Composites), Brenda Wistor-Linfield, and Chris Wyszkowski.

References

[1] Aaron, K. M., "Balloon Trajectory Control System," U.S. Patent No. 6,402,090, filed 29 June 1998, issued 11 June 2002.

[2] Randel, W. J., "Global Atmospheric Circulation Statistics, 1000-1 MB," National Center for Atmospheric Research, Rept. TN-366+STR, Boulder, CO, Feb. 1992.

[3] Sheldal, R. E., and Klimas, P. C., "Aerodynamic Characteristics of Seven Airfoil Sections Through 180 Degrees Angle of Attack for Use in Aerodynamic Analysis of Vertical Axis Wind Turbines," Sandia National Labs., Rept. SAND80-2114, Albuquerque, NM, Mar. 1981.

[4] Albertson, J. A., Troutt, T. R., Siuru, W. D., and Walker, J. M., "Dynamic Stall Vortex Development and the Surface Pressure Field of a Pitching Airfoil," AIAA 19th Fluid Dynamics, Plasma Dynamics and Lasers Conference, Honolulu, HI, AIAA Paper 87-1333, June 1987.

[5] Conger, R. N., and Ramaprian, B. R., "Pressure Measurements on a Pitching Airfoil in a Water Channel," *AIAA Journal*, Vol. 32, No. 1, Jan. 1994, pp. 108–115.

[6] Corke, T. C., He, C., and Patel, M. P., "Plasma Flaps and Slats: An Application of Weakly-Ionized Plasma Actuators," 2nd AIAA Flow Control Conference, Portland, OR, AIAA Paper 2004-2127, 28 June–1 July 2004.

[7] Greenblatt, D., and Wygnanski, I., "The Control of Flow Separation by Periodic Excitation," *Progress in Aerospace Sciences*, Vol. 36, 2000, pp. 487–545.
doi:10.1016/S0376-0421(00)00008-7

[8] Greenblatt, D., and Wygnanski, I., "Dynamic Stall Control by Periodic Excitation, Part 1: NACA 0015 Parametric Study," *Journal of Aircraft*, Vol. 38, No. 3, pp. 430–438, May–June 2001.

[9] Jumper, E. J., Schreck, S. J., and Dimmick, R. L., "Lift-Curve Characteristics for an Airfoil Pitching at Constant Rate," *Journal of Aircraft*, Vol. 24, No. 10, Oct. 1987, pp. 680–687.

[10] Mangalam, A. S., and Moes, T. R., "Real-Time Unsteady Load Measurements Using Hot-Film Sensors," 22nd Applied Aerodynamics Conference and Exhibit, Providence, RI, AIAA Paper 2004-5371, 16–19 August 2004.

[11] Tuck, A., and Soria, J., "Active Flow Control over a NACA 0015 Airfoil Using a ZNMF Jet," 15th Australasian Fluid Mechanics Conference, Sydney, Australia, Univ. of Sydney Paper 178, 13–17 Dec. 2004.

[12] Weier, T., and Gerbeth, G., "Control of Separated Flows by Time Periodic Lorentz Forces," *European Journal of Mechanics, B/Fluids*, Vol. 23, No. 6, 2004, pp. 835–849.

doi:10.1016/j.euromechflu.2004.04.004
[13] Wygnanski, I., and Seifert, A., "The Control of Separation by Periodic Oscillations," 18th AIAA Aerospace Ground Testing Conference, Colorado Springs, CO, AIAA Paper 94-2608, 20–23 June 1994.
[14] Yon, S. A., and Katz, J., "Study of the Unsteady Flow Features on a Stalled Wing," *AIAA Journal*, Vol. 36, No. 3, Mar. 1998, pp. 305–312.
[15] Elkaim, G., "System Identification for Precision Control of a Wingsailed GPS-Guided Catamaran," Ph.D. Thesis, Stanford Univ., Palo Alto, CA, Dec. 2001.
[16] Hazen, N. L., and Anderson, J. G., "Reel Down: A Balloon-Borne Winch System for Stratospheric Sounding from Above," 22nd AIAA Aerospace Sciences Meeting, Reno, NV, AIAA Paper 84-0027, 9–12 Jan. 1984.
[17] Hazen, N. L., and Anderson, J. G., "A New Reeling Technique for Very Long Extension Scanning in the Stratosphere," *Advances in Space Research*, Vol. 5, No. 1, 1985, pp. 45–48. doi:10.1016/0273-1177(85)90422-3
[18] Nock, K. T., Heun, M. K., and Aaron, K. M., "Global Stratospheric Balloon Constellations," *Advances in Space Research*, Vol. 30, No. 5, 2002, pp. 1233–1238. doi:10.1016/S0273-1177(02)00528-8
[19] Nock, K. T., Heun, M. K., and Aaron, K. M., "Global Constellations of Stratospheric Satellites," *15th ESA Symposium on European Rocket and Balloon Programmes & Related Research*, SP-471, ESA, Paris, May 2001, pp. 663668.